JACS
JOURNAL OF THE AMERICAN CHEMICAL SOCIETY
Article
pubs.acs.org/JACS

^{15}N Magnetic Resonance Hyperpolarization via the Reaction of Parahydrogen with ^{15}N-Propargylcholine

Francesca Reineri,[†] Alessandra Viale,[†] Silvano Ellena,[†] Diego Alberti,[†] Tommaso Boi,[†] Giovanni Battista Giovenzana,[‡] Roberto Gobetto,[†] Samuel S. D. Premkumar,[†] and Silvio Aime*[,†]

[†]Dipartimento di Chimica IFM, University of Torino, V. P. Giuria 7, 10125 Torino, Italy

[‡]DiSCAFF & DFB Center, Università degli Studi del Piemonte Orientale "A. Avogadro", Via Bovio 6, I-28100 Novara, Italy

Supporting Information

ABSTRACT: ^{15}N-Propargylcholine has been synthesized and hydrogenated with para-H_2. Through the application of a field cycling procedure, parahydrogen spin order is transferred to the ^{15}N resonance. Among the different isomers formed upon hydrogenation of ^{15}N-propargylcholine, only the nontransposed derivative contributes to the observed N-15 enhanced emission signal. The parahydrogen-induced polarization factor is about 3000. The precise identification of the isomer responsible for the observed ^{15}N enhancement has been attained through a retro-INEPT (^{15}N−^{1}H) experiment. T_1 of the hyperpolarized ^{15}N resonance has been estimated to be ca. 150 s, i.e., similar to that reported for the parent propargylcholine (144 s). Experimental results are accompanied by theoretical calculations that stress the role of scalar coupling constants (J_{HN} and J_{HH}) and of the field dependence in the formation of the observed ^{15}N polarized signal. Insights into the good cellular uptake of the compound have been gained.

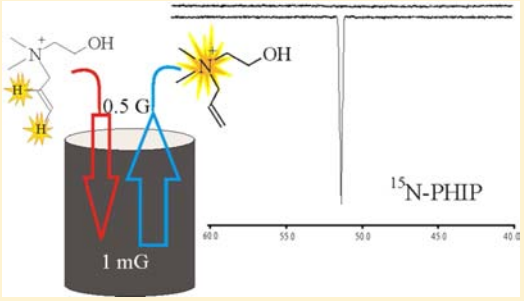

INTRODUCTION

Magnetic resonance hyperpolarization techniques are under intense scrutiny as the possibility of overcoming the sensitivity limitations may open a number of innovative applications, in chemistry and biology. The driving force is represented by the development of highly innovative magnetic resonance imaging (MRI) procedures based on the detection of key metabolites that directly report on the specific steps of cellular machinery (metabolic imaging). Polarized states lifetime is determined by relaxation rate of the involved resonance and only functionalities characterized by long relaxation time are useful for these applications.[1−4] ^{13}C resonances, usually belonging to carbonyl groups in small-sized molecules, have been considered because representatives of this class of molecules are easily formed in key metabolic pathways.[5−7] To now ^{13}C-pyruvate is the most used substrate, being a key chemical in the TCA metabolic pathway, and the detection of its transformation allows one to obtain information about the deviation from the healthy state, at the cellular level.[8]

Among the other low γ heteronuclei particularly important in biological systems, ^{15}N is the most appealing one, since it is often characterized by a very long relaxation time thanks to the highly symmetrical environment it often owns in the molecules of interest.

Up to now, few ^{15}N-containing substrates have been hyperpolarized, namely, ^{15}N-urea,[9] some amino acids,[10] and, most importantly, due to its long T_1 value (120 s), ^{15}N-choline.[11−14] All these molecules have been polarized by the DNP method. To the best of our knowledge, ^{15}N hyperpolarization with parahydrogen has been achieved on pyridine only, by means of the SABRE method,[15] while no examples of ^{15}N hyperpolarization by parahydrogen induced polarization (PHIP)[16] on biocompatible substrates have been reported.

The possibility of generating ^{15}N hyperpolarized resonances that can be used for in vivo studies by means of PHIP procedure would be outstandingly interesting. The major limitation appears related to the availability of α-unsaturated substrates that, upon hydrogenation, would bring the added parahydrogen protons two and three bonds away from the ^{15}N center. Unfortunately, the hydrogenation of such systems invariantly leads to the cleavage of the N−C bond and the release of the hydrogenated moiety. Thus, one has to turn to molecules containing an sp^3 carbon between the unsaturated group and the ^{15}N atom. To test the feasibility of ^{15}N hyperpolarization for molecules containing the latter structural arrangement, the propargylcholine derivative **1** has been synthesized and its reaction with parahydrogen has been tested. Compound **1** mimics the parent choline molecule and it might have potential in vivo applications.

RESULTS AND DISCUSSION

Synthesis and Characterization of *N*-Propargylcholine (1). *N*-Propargylcholine tosylate was prepared by the synthetic procedure depicted in Scheme 1. First 2-hydroxyethanolamine was methylated by reaction with formaldehyde and formic acid, and then *N*,*N*-dimethylethanolamine was reacted with prop-

Received: October 20, 2011
Published: June 4, 2012

   dx.doi.org/10.1021/ja209884h | J. Am. Chem. Soc. 2012, 134, 11146−11152

Chart 1. *N*-Propargylcholine Tosylate

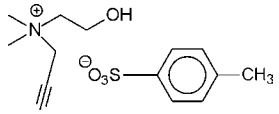

Scheme 1. Synthetic Procedure for the Preparation of Deuterated ^{15}N-Propargylcholine

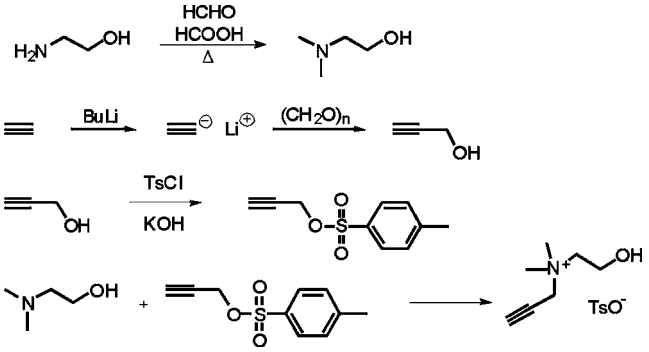

argyltosylate to yield *N*-propargylcholine. For the preparation of the ^{15}N-enriched compound, ^{15}N-ethanolamine was used. Deuteration of the methylenic group adjacent to the nitrogen atom was achieved by using deuterated propargyltosylate, which was synthesized by reaction of lithium monoacetylide with deuterated paraformaldehyde to yield deuterated propargyl alcohol. The successive reaction of the alcohol with tosyl chloride yields a product well-suitable for the hydrogenation reaction to be carried out either in water or in organic solvent.

^{15}N T_1 measurements showed that, as for choline, the quaternary nitrogen atom is characterized by a very long T_1 (104 s in water at 14 T). Deuteration of the adjacent methylenic group caused a further T_1 increase to 144 s. On the basis of the close similarity between the nitrogen surrounding in *N*-propagylcholine and its hydrogenated product, it is surmised that the latter would show similar relaxation times. Such long relaxation time is a really favorable parameter for development of MRI protocols based on the use of the hyperpolarized choline derivative, since it guarantees that both parahydrogenation and further handlings can be carried out without significant polarization loss.

Hydrogenation of *N*-Propargylcholine (1). Hydrogenation of *N*-propargylcholine (**1**), carried out either in a mixture of acetone and methanol or in water, catalyzed by [Rh(diphenylphosphinobutane)(cyclooctadiene)][BF_4] and [Rh(1,4-bis[(phenyl-3-propanesulfonate)phosphine]butane)-(norbornadiene)][BF_4] catalysts, respectively affords five different products (Scheme 2, Figure 1). Their characterization has been pursued by NMR spectroscopy by means of ^{1}H-COSY and ^{1}H−^{15}N HMBC experiments.

Compound **a** is the main product (about 45%) of both experimental conditions. **b** and **b′** derivatives are formed by transposition of the double bond from **a**, resulting in the cis (**b′**) and trans (**b**) isomers of the alkene in which the olefin is adjacent to N. Due to the intrinsic instability of such configuration, **b** and **b′** partially undergo propargyl elimination, yielding dimethylethanolamine and partially deuterated $CH_3CH_2CH(OCH_3)_2$ (in acetone/CD_3OD) or CH_3CH_2CHO (in D_2O). The fifth reaction product (**c**) corresponds to the complete hydrogenation of the substrate (about 10%).

Scheme 2. Hydrogenation of *N*-Propagylcholine Affords Five Products[a]

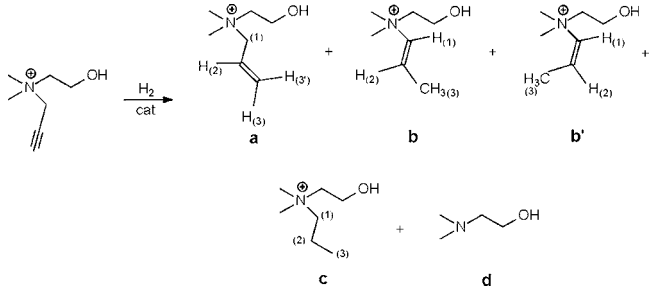

[a]Compound **a** is formed at the higher yields (45%).

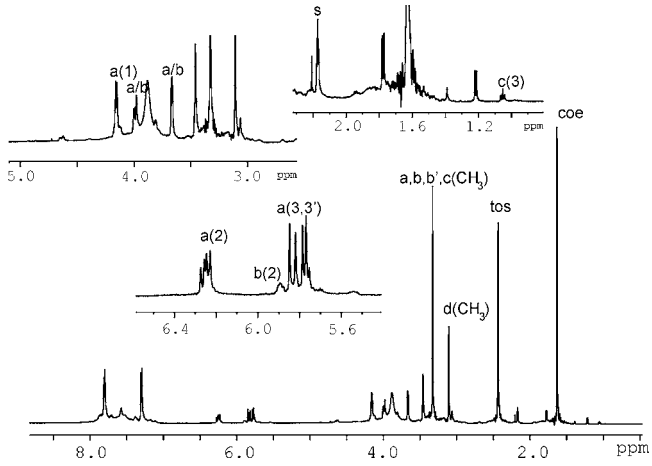

Figure 1. ^{1}H NMR spectrum of the products deriving from the hydrogenation of *N*-propargylcholine [acetone-d_6/CD_3OD 4:1, room temperature (RT), 9.4 T]. tos = tosylate; coe = cyclooctene; s = solvent.

More insight into the transposition path was gained by acquiring ^{2}H NMR spectrum of the products of the reaction between *N*-propargylcholine and D_2. Deuterium incorporation in **b**/**b′** has been observed only at the 2- and 3-positions to indicate that the added deuterons are not involved in the transposition process. Thus, the process deals with the transfer of one of the two H(1) to the 3-position. This may take place immediately after the hydrogenation reaction, while the just formed alkene is still coordinated to the metal complex, via a π-allyl intermediate as depicted in Scheme 3.[17] A carbene-mediated mechanism can be ruled out since it would yield incorporation of both the deuterons on the 3-position.

PHIP Effects in the ^{1}H NMR Spectrum. PHIP effects have been observed in the ^{1}H spectrum upon reaction with parahydrogen of *N*-propargylcholine. The absorption/emission pattern is similar for the three considered isotopomers (i.e., *N*-

Scheme 3. Double Bond Transposition Leading from a to b/b′

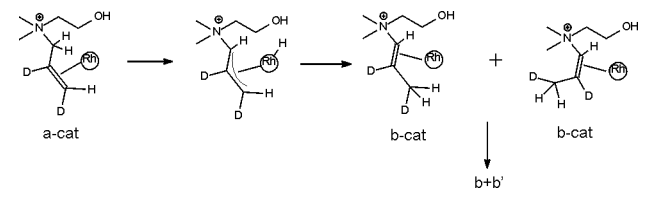

dx.doi.org/10.1021/ja209884h | J. Am. Chem. Soc. 2012, 134, 11146−11152

propargylcholine, ^{15}N-labeled *N*-propargylcholine, and deuterated, ^{15}N-labeled *N*-propargylcholine) and does not change upon passing from organic solvent to water.

The ^{1}H-spectrum of the products obtained from the reaction of *N*-propargylcholine with para-H_2 in acetone-d_6/CD_3OD is reported in Figure 2. It clearly shows enhanced signals for **a**, **b**, **b′**, and **c** products. Among them, the most intense ^{1}H-PHIP effects are those ones arising from **b**/**b′**, in spite of their lower concentration. From the transposition mechanism it derives that on product **b**/**b′** parahydrogen protons are added in positions 3 and 2, and then polarization is transferred to the methyl protons. Therefore, the highest proton polarization is observed on the methyl signal.

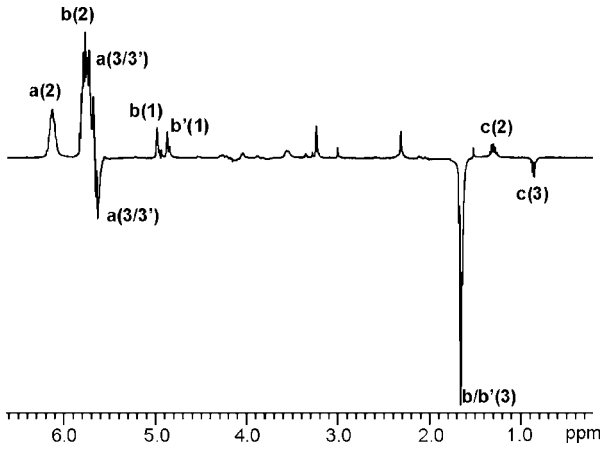

Figure 2. ^{1}H NMR spectrum of the products of the reaction of *N*-propargylcholine with para-H_2 (one scan, RT, acetone-d_6/CD_3OD 4:1, 9.4 T).

^{15}N-PHIP. It is well-established that hyperpolarization is transferred from parahydrogen to heteronuclei through scalar coupling.[18] Polarized spin order $I_z^H I_z^N$ can be directly obtained in parahydrogenation experiments, and enhancement is a function of the ratio $R = (J_{NH} - J_{NH'})/J_{HH'}$, where H and H′ are the two parahydrogen protons, H being the most strongly coupled with ^{15}N. As can be observed in Figure 3a, the heteronuclear polarization (P) is null when the two protons experience the same coupling with the heteroatom, it tends to zero when J coupling between the two protons vanishes, and it is a maximum for $(J_{NH} - J_{NH'})/J_{HH'} \approx \sqrt{8}$, in accordance with that reported earlier by Bargon et al.[18] Scalar coupling values between parahydrogen protons and nitrogen in the observed reaction products are all quite small. The protons in the 3-position (Scheme 2) are four bonds away from the nitrogen nucleus and their J coupling value with ^{15}N can be approximated to zero. The protons in the 2-position experience a $^{3}J_{HN}$ coupling that is about 2 Hz for **b′**-like systems, having a trans configuration, 3 Hz for **a**-like systems, and 5 Hz for **b**-like systems, having cis configuration.[12,19] It has also been reported that ^{2}J coupling between ^{15}N and ^{1}H are smaller than 1 Hz.[14] On this basis it can easily be shown that the expected enhancement on ^{15}N would be much smaller than the one usually observed on ^{13}C. As reported in Figure 3b the maximum theoretical enhancement attainable on ^{15}N is expected to be 1 order of magnitude lower than the one observed on ^{13}C. Moreover, the splitting between the absorption and emission peaks is smaller, thus contributing to the mutual cancellation of the two polarized peaks. As a matter of fact, no ^{15}N-polarization was observed following a parahydrogenation ALTADENA experiment.[16,20]

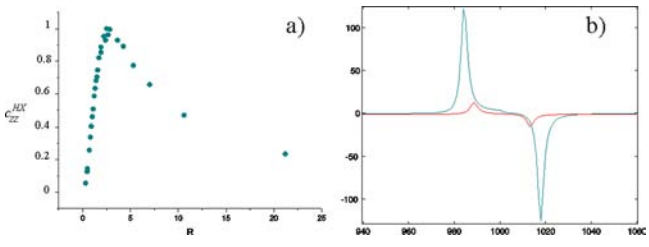

Figure 3. (a) Polarization transfer to proton-heteronucleus spin order $I_z^H I_z^X$ as a function of coefficient $R = |J_{HX} - J_{H'X}|/J_{HH'}$. (b) c_{zz}^{HX} comparison between maximum theoretical enhancement that can be achieved on a nucleus X for which $R = 1.7$ (corresponding to $c_{zz}^{HX} = 0.8$; blue line) and another with $R = 0.2$ (corresponding to $c_{zz}^{HX} = 0.08$; red line). The first is related to J coupling values typical of a carbonyl group adjacent to double bond, the second one is obtained using J coupling values of propargylcholine hydrogenation product **a**.

It is also well-established[21] that heteronuclear hyperpolarization can be manipulated by low magnetic field cycle. This procedure is based on the fact that at 0.5 G (earth field) the Larmor frequencies of magnetically active nuclei are still different, so the weak coupling condition between heteroatoms applies. On the contrary, when the magnetic field is further lowered to 1 mG, isotropic mixing between all the magnetically active nuclei is obtained.

The variations of the spin states populations during field cycle can be treated using the product operator formalism and a three spins system (HH′X). This system is quite a simplification of the real spin systems, as it does not take into account all the protons of the product molecules. However, it allows one to demonstrate how polarization intensity of the heteronucleus can be changed upon field cycle application.

It has already been reported that, after parahydrogen addition to a molecule, the parahydrogen density operator is perturbed and then a new steady state is reached.[22] The present study starts from the steady-state condition which is obtained on an HH′X spin system when the reaction with parahydrogen is carried out at the earth magnetic field (EF)[22]

$$\sigma_{EF} = E/4 + c_{ZZ_{HH'}}^{EF} I_z^H I_z^{H'} + c_{(ZQ_{HH'})_x}^{EF} (ZQ_{HH'})_x + c_{(ZQ_{HH'})_y}^{EF} (ZQ_{HH'})_y + c_{ZZ_{HX}}^{EF} (I_z^H - I_z^{H'}) I_z^X \quad (1)$$

where $ZQ_{HH'}$ is zero quantum coherence between the two protons.

When the magnetic field is nonadiabatically lowered (nearly 1 mG), the equilibrium state is suddenly perturbed by the fully coupled Hamiltonian (ZF denoting zero field)

$$\hat{H}_{ZF} = -\nu_H (I_z^H + I_z^{H'}) - \nu_N I_z^X + J_{HH'} [I_z^H I_z^{H'} + ZQ_x^{HH'}] + J_{HX} [I_z^H I_z^X + ZQ_x^{HX}] + J_{H'X} [I_z^{H'} I_z^X + ZQ_x^{H'X}] \quad (2)$$

after which a new steady state is reached

dx.doi.org/10.1021/ja209884h | J. Am. Chem. Soc. 2012, 134, 11146−11152

$$\sigma_{ZF} = E/4 + c_{zz}^{HH'} I_z^H I_z^{H'} + c_{ZQ_x}^{HH'} (ZQ_{HH'})_x + c_{ZQ_y}^{HH'} (ZQ_{HH'})_y c_{zz}^{HX} I_z^H I_z^X + c_{ZQ_x}^{HX} (ZQ_{HX})_x + c_{ZQ_y}^{HX} (ZQ_{HX})_y + c_{zz}^{H'X} I_z^{H'} I_z^X + c_{ZQ_x}^{H'X} (ZQ_{H'X}) + c_{ZQ_y}^{H'X} (ZQ_{H'X})_y + c_z^H (I_z^H - I_z^{H'}) + c_z^X I_z^X \quad (3)$$

All the c coefficients are a function of J coupling and of the frequency difference between ^{1}H and the heteronucleus, which is related to the magnetic field strength. In our case, the amount of longitudinal magnetization on ^{15}N (coefficient c_z^N) has been calculated as a function of magnetic field (Figure 4).

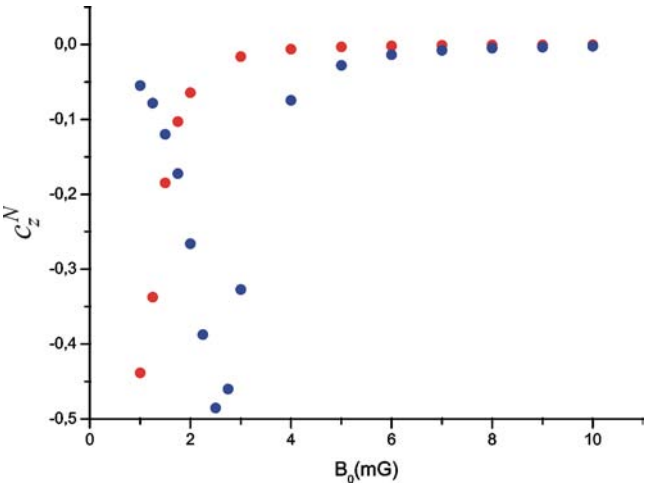

Figure 4. The amount of longitudinal magnetization (c_z^N) at very low magnetic field (from 1 to 10mG) as a function of the magnetic field strength. These values have been calculated for product **a** (blue circles) and product **b** (red) having (a) J_{HH} = 10 Hz, J_{HN} = 3 Hz, $J_{H'N}$ = 0 Hz and (b) J_{HH} = 4 Hz, J_{HN} = 2 Hz, $J_{H'N}$ = 0 Hz, respectively.

After that the steady-state condition at zero field has been reached (a few seconds), the magnetic field shield is slowly (adiabatically) removed. During this adiabatic passage from zero to earth field the density operator is subjected to a time-dependent Hamiltonian

$$\hat{H}(t) = -\nu_H(t)(I_z^H + I_z^{H'}) - \nu_X(t) I_z^X + J_{HH} \mathbf{I_H} \mathbf{I_{H'}} + J_{HX} \mathbf{I_H} \mathbf{I_X} + J_{H'X} \mathbf{I_{H'}} \mathbf{I_X} \quad (4)$$

where the Larmor frequencies are time-dependent while J coupling is constant.

Density matrix during the adiabatic passage has been numerically calculated by applying a time-dependent Liouville–Von Neumann equation

$$\sigma(t+\Delta t) = \exp(-2i\pi \hat{H}_{(t+\Delta t)} \Delta t) \sigma(t) \exp(2i\pi \hat{H}_{(t+\Delta t)} \Delta t) \quad (5)$$

From the calculated time-dependent density operator, longitudinal magnetization of the heteronucleus, represented by the coefficient c_z^N, has been extracted and reported as a function of time (Figure 5).

Simulations of the adiabatic transport have been carried out for molecule **a**. If the starting magnetic field is zero, it can be derived from Figure 4 that the absolute value of longitudinal magnetization on 15N is minimum. In this case, the amount of longitudinal magnetization obtained at the end of transport

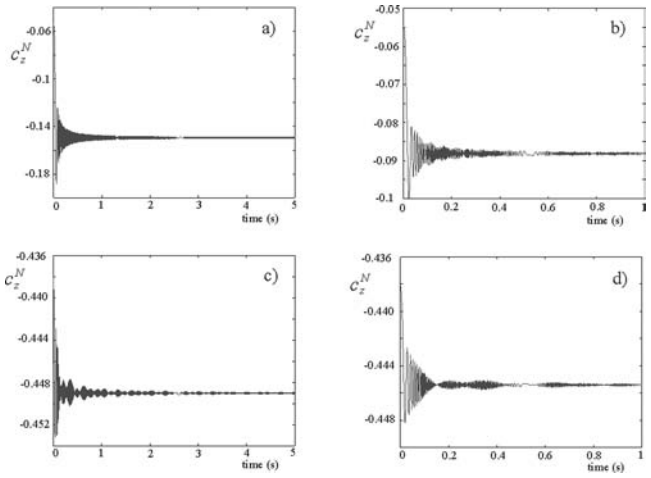

Figure 5. c_z^N as a function of transport time from 1 to 500 mG. Molecule **a** (J_{HH} = 10 Hz, J_{HN} = 3 Hz, $J_{H'N}$ = 0) was used for these simulations. Diagrams were obtained starting from 0 mG: (a) slow transport (5 s), $\langle c_z^N \rangle_{B=0.5G} = -0.15$; (b) fast transport (1 s) $\langle c_z^N \rangle_{B=0.5G} = -0.09$. Diagrams were calculated starting from 2.5 mG: (c) slow transport (5 s) $\langle c_z^N \rangle_{B=0.5G} = -0.45$; (d) fast transport (1 s) $\langle c_z^N \rangle_{B=0.5G} = -0.45$.

(500 mG, earth field) is strongly dependent on the speed of transport. In fact, it can be observed from Figure 5 that, if transport takes 5 s instead of 1 s, the absolute value of c_z^N is almost doubled. On the contrary, if the starting B_0 coincides with that at which heteronuclear magnetization is a maximum (2.5 mG for molecule **a**), the speed of transport does not influence the amount of longitudinal ^{15}N magnetization, the value of which remains close to that achieved at low field.

It is evident that, in order to optimize the amount of longitudinal polarization on the heteronucleus, the magnetic field strength must be exactly measured; that is not a trivial task in the μ-metal cylinder that has been used for our measurements. However, is important to notice that longitudinal polarization (I_z^N) is, in all these cases, higher than the calculated value of polarized spin order (c_{zz}^{HN}).

Following the application of field cycle to parahydrogenated ^{15}N-propargylcholine, polarized ^{15}N is indeed obtained (Figure 6).

The chemical shift of the enhanced peak (56.34 ppm) does not allow one to discriminate whether it pertains to **a** and/or **b**/**b**′ and/or **c**. Furthermore, as the magnetic field strength into the μ-metal cylinder is not exactly known, it is not possible to know, in principle, which is the most polarized molecule. Surely, the ^{15}N signal for **d** (36.36 ppm) is not polarized. Because of the very small difference between the ^{15}N chemical shifts of **a**, **b**/**b**′, and **c**, it is not possible to distinguish which of the different species leads to the observed heteronuclear polarization. To tackle this task the selective inverse INEPT sequence has been applied to the parahydrogenated products. This experiment allows one to identify those protons that are scalarly coupled to the polarized ^{15}N nucleus.[12] In the resulting spectrum (Figure 7), all the signals related to **a** are present, while no signal can be observed for **b**/**b**′ and **c**. This finding clearly indicates that the polarization transfer yielding the ^{15}N enhancement has occurred mainly in **a**.

The longitudinal relaxation time of molecule **a** has been estimated by following the ^{15}N polarization decay upon the application of small flip angles to acquire the enhanced signals

dx.doi.org/10.1021/ja209884h | J. Am. Chem. Soc. 2012, 134, 11146–11152

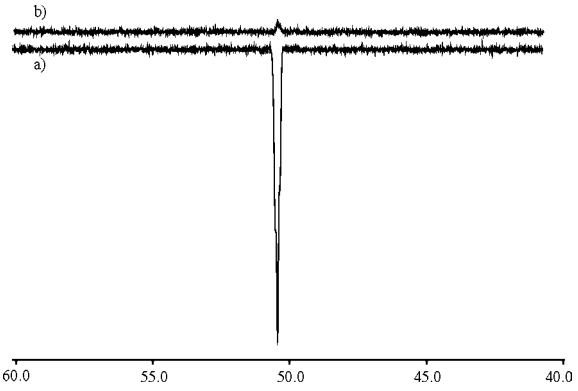

Figure 6. ^{15}N spectrum of parahydrogenated ^{15}N-propargylcholine. (a) single-scan spectrum recorded immediately after parahydrogenation and field cycling and (b) 80-scan spectrum recorded after relaxation (acetone-d_6/CD_3OD 4:1, RT, 9.4 T). The signal enhancement is about 3000 times. As the magnetic field profile is not exactly known inside the cylinder, polarization may be further increased by using an electromagnetic field shield.

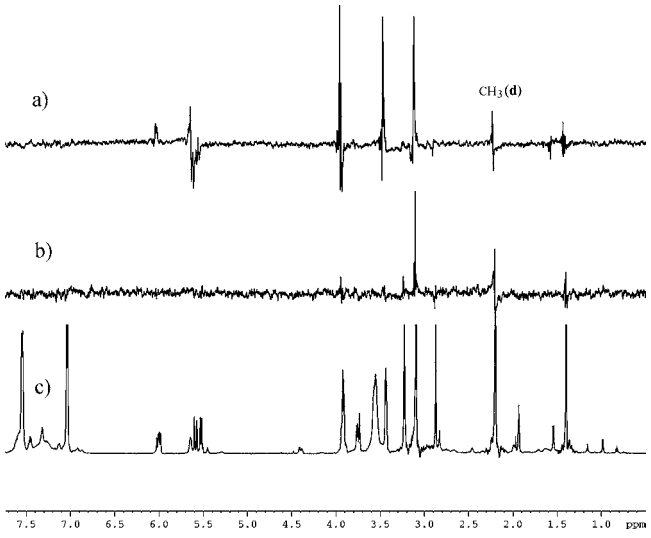

Figure 7. Inverse INEPT spectra of parahydrogenated ^{15}N-propargicholine-d_2. (a) Inverse INEPT spectrum of the ^{15}N hyperpolarized molecule: signals from H(2) and H(3), methylic and methylenic protons of product **a**; (b) inverse INEPT spectrum recorded after ^{15}N polarization has returned to equilibrium; (c) standard ^{1}H NMR single-scan spectrum at equilibrium (acetone-d_6/CD_3OD 4:1, RT, 14 T).

at various time intervals. This procedure afforded a T_1 value of ca. 140 s, which is similar to that measured for the starting alkyne molecule, as expected.

In Vitro Essays on Cell Cultures. In order to get some more insights into the potential of ^{15}N-propargylcholine for further in vivo imaging studies, we went to carry out cellular uptake experiments using the hydrogenation product mixture containing **a** (45%), **b** and **b′** (24%), **c** (9%), and **d** (20%).

Breast cancer cells (MCF7) have been chosen for this experiment, as it has been reported[23] that either choline transport and choline kinase activity is up-regulated in this tumor cell line. Moreover, it has also been demonstrated that the rate of choline phosphorylation, in these cells, is more than 2 orders of magnitude faster than the rate of transport.

Uptake experiments were carried out on cells seeded in 60 mm Pedri dishes and incubated with different concentrations of the hydrogenation product mixture (15, 0.95, and 0.36 mM) for time lags increasing from 10 to 480 min. Figure 8 reports a

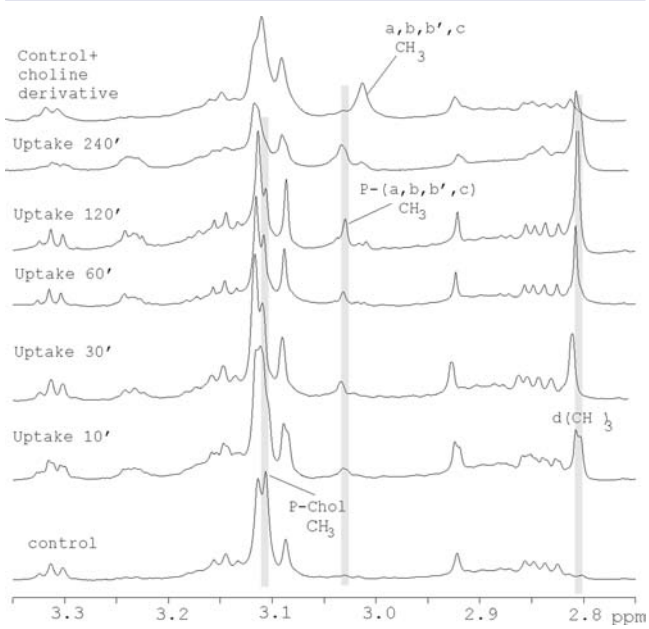

Figure 8. Cellular uptake of hydrogenation products derived from parahydrogenation of propargylcholine (1 mM total concentration of product molecules). Bottom spectrum: MCF-7 cells extract in normal grow medium. Top spectrum: cells extract after the addition of the mixture of choline derivatives added to the medium. Middle spectra: cell extracts at increasing incubation time. Methyl signals of phosphocholine and its parent compounds are indicated with P-Chol and P-(a,b,b′,c).

selection of ^{1}H NMR spectra of cellular extracts to summarize the results of the cellular uptake experiments. Upon increasing the incubation time, the progressive growth of a peak at 3.03 ppm is observed. This peak is not present in the control ^{1}H NMR spectrum corresponding to cell lysate. In the latter solution (top trace in Figure 8), the methyl signal of **a**, **b**, **b′**, and **c** is detected at 3.01 ppm when the hydrogenation products mixture is added. A peak at 3.01 ppm is also observed at long incubation times (see fifth and sixth traces from bottom in Figure 8). On this basis, the peak at 3.03 ppm has been assigned to the phosphocholine derivatives of the **a**, **b**, **b′**, **c** choline mimics mixture (the chemical shift separation is the same order of magnitude as that observed between choline and phosphocholine, at 3.08 and 3.10 ppm, respectively; see the Supporting Information). The observed behavior indicates that, upon entering the cells, the **a**, **b**, **b′**, **c** choline mimics are readily phosphorilated and only at later times the signal for the unphopshorilated derivatives is detected.[23]

Although the methyl signal is the same for all the molecules derived from hydrogenation of propargylcholine, the percentage of compound **a** with respect to other hydrogenation products can be derived from the intensity of the olefinic signal at 5.47 ppm with respect to the methyl one (see Supporting Information). From this comparison one may draw the conclusion that the relative percentage of this compound is maintained in the cells extract, thus suggesting that the uptake of all the hydrogenation products takes place at about the same rate.

The amount of compound **a** taken up by cells is reported in Figure 9. From these data, using the values obtained for [**a**] =

dx.doi.org/10.1021/ja209884h | J. Am. Chem. Soc. 2012, 134, 11146−11152

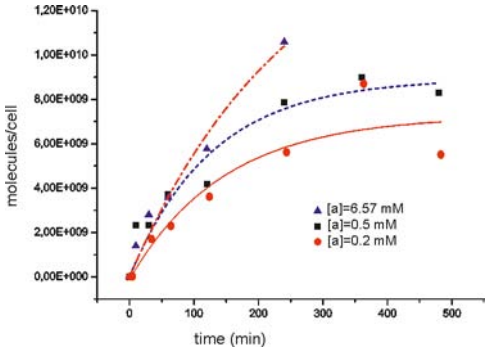

Figure 9. MCF-7 uptake experiments. Although the experiments have been carried out using the **a**, **b**, **b′**, **c** hydrogenation products mixture, the reported quantities (in molecules/cell) refers to compound **a** (45% in the hydrogenation mixture, see text). Dashed-dotted line, triangles [**a**] = 6.57 mM; dashed line and squares, [**a**] = 0.5 mM; straight line and dots, [**a**] = 0.2 mM.

0.5 mM, it can be derived that, after 1 min, the concentration of internalized **a** is 1×10^8 molecules/cell. In solid tissues, the number of cells/mL is on the order of 3×10^8; thus, compound **a** reaches the concentration of 0.5 mM after 1 min. Considering that the attainable polarization is 3000 times and that the relaxation rate is 140 s, after 1 min enhancement is about 1900 times. As a solution containing 1 M ^{15}N-choline gives a S/N of 10, we can say that the amount of internalized **a** is enough to be observed using the hyperpolarized product.

The cellular uptake of compound a appears to be effected, to some extent, by the concentration of the choline in the incubation medium. Figure 10 shows that, when [**a**] = 0.2 mM

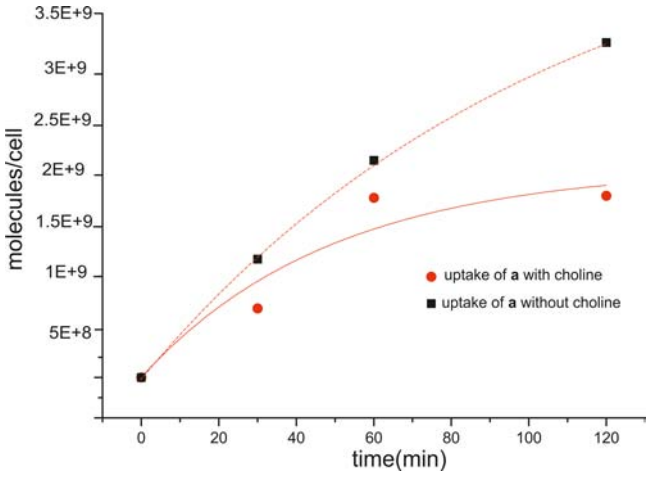

Figure 10. Straight line, dots: cellular uptake rate of **a** ([**a**] = 0.2 mM) incubated with choline (0.3 mM) in the grow medium. Dashed line, squares: cellular uptake with [**a**] = 0.2 mM, without choline.

and [choline] = 0.3 mM, the observed uptake of **a** is significantly decreased. Thus, one may conclude that **a** enters into MCF-7 cells by means of the same transporters used by choline.[24]

CONCLUSIONS

This work has shown that it is possible to hyperpolarize the ^{15}N resonance of an unsaturated derivative of choline by reaction with parahydrogen if the spin order derived from parahydrogen is changed into net ^{15}N polarization by magnetic field cycling between earth and zero field. Among the different isomeric structures that form upon hydrogenation of propargylcholine, it has been shown that only one molecule (**a**, Scheme 1) is effectively ^{15}N polarized under the employed experimental setup. Its identification has been possible through a retro-INEPT experiment that has allowed polarization transfer from ^{15}N to the ^{1}H resonances.

In the investigated system the ^{15}N resonance maintains a very long T_1 value in analogy with that previously reported for the parent choline.

Cellular uptake experiments have demonstrated that internalization of the choline derivatives takes place by the same membrane transporters as choline. Furthermore, the concentration of the polarized molecule **a** has been evaluated to be enough to be observed in tissues and in particular in breast cancer cells, for which the altered choline metabolism and uptake have been previously demonstrated.

ASSOCIATED CONTENT

Supporting Information

Experimental procedures, synthesis of substrate molecules, and calculations of the time-dependent density operator during field cycling using an on-purpose function written with Matlab 7.0. This material is available free of charge via the Internet at http://pubs.acs.org.

AUTHOR INFORMATION

Corresponding Author

silvio.aime@unito.it

Notes

The authors declare no competing financial interest.

ACKNOWLEDGMENTS

We gratefully acknowledge Regione Piemonte (bando POR-FESR 2007, Asse 1, Misura I.1.1) for financial support.

REFERENCES

(1) Mansson, S.; Johansson, E.; Magnusson, P.; Chai, C. M.; Hansson, G.; Petersson, J. S.; Stahlberg, F.; Golman, K. *Eur. Radiol.* **2006**, *16*, 57−67 and references therein.

(2) Viale, A.; Reineri, F.; Santelia, D.; Ellena, S.; Gobetto, R.; Aime, S. *Q. J. Nucl. Med. Mol. Imag.* **2009**, *53*, 604−617 and references therein.

(3) Viale, A.; Aime, S. *Curr. Op. Chem. Biol.* **2010**, *14*, 90−96 and references therein..

(4) Gallagher, F. A.; Kettunen, M. I.; Brindle, K. M. *Prog. Nucl. Magn. Reson. Spectrosc.* **2009**, *55*, 285−295 and references therein.

(5) Kohler, S. J.; Yen, Y.; Wolber, J.; Chen, A. P.; Albers, M. J.; Bok, R.; Zhang, V.; Trop, J.; Nelson, S.; Vigneron, D. B.; Kurhanewicz, J.; Hurd, R. E. *Magn. Res. Med.* **2007**, *58*, 65−69.

(6) Nelson, S. J.; Vigneron, D.; Kurhanewicz, J.; Chen, A.; Bok, R.; Hurd, R. *Appl. Magn. Reson.* **2008**, *34*, 533−544.

(7) (a) Chekmenev, E. Y.; Hovener, J.; Norton, V. A.; Harris, K.; Batchelder, L. S.; Bhattacharya, P.; Ross, B. D.; Weitekamp, D. P. *J. Am. Chem. Soc.* **2008**, *130*, 4212−4213. (b) Reineri, F.; Viale, A.; Ellena, S.; Boi, T.; Daniele, V.; Gobetto, R.; Aime, S. *Angew. Chem., Int. Ed.* **2011**, *32*, 7350−7353.

(8) Albers, M. J.; Bok, R.; Chen, A. P.; Cunningham, C. H.; Zierhut, M. L.; Yi Zhang, V.; Kohler, S. J.; Tropp, J.; Hurd, R. E.; Yen, Y.; Nelson, S. J.; Vigneron, D. B.; Kurhanewicz, J. *Cancer Res.* **2008**, *68*, 8607−8615.

(9) Golman, K.; Ardenkjaer-Larsen, J. H.; Petersson, J. S.; Mansson, S.; Leunbach, I. *Proc. Natl. Acad. Sci. U. S. A.* **2003**, *100*, 10435−10439.

(10) Hall, D. A.; Maus, D. C.; Gerfen, G. J.; Inati, S. J.; Becerra, L. R.; Dahlquist, F. W.; Griffin, R. G. *Science* **1997**, *276*, 930−932.

(11) Cudalbu, C.; Comment, A.; Kurdzesau, F.; van Heeswijk, R. B.; Jannin, S.; Denisov, V.; Zirik, D.; Gruetter, R. *Phys. Chem. Chem. Phys.* **2010**, *15*, 5818−5823.
(12) Gabellieri, C.; Reynolds, S.; Lavie, A.; Payne, G. S.; Leach, M. O.; Eykyn, T. R. *J. Am. Chem. Soc.* **2008**, *130*, 4598−4599.
(13) Sarkar, R.; Comment, A.; Vasos, P. R.; Jannin, S.; Gruetter, R.; Bodenhausen, G.; Hall, H.; Kirik, D.; Denisov, V. P. *J. Am. Chem. Soc.* **2009**, *131*, 16014−16015.
(14) Pfeilstikcer, J. A.; Ollerenshw, J. E.; Norton, V. A.; Weitekamp, D. P. *J. Magn. Reson.* **2010**, *205*, 125−129.
(15) Adams, R. W.; Aguilar, J. A.; Atkinson, K. D.; Cowley, M. J.; Elliott, P. I.; Duckett, S. B.; Green, G. G.; Khazal, I. G.; López-Serrano, J.; Williamson, D. C. *Science* **2009**, *323*, 1708−1711.
(16) Natterer, J.; Bargon. *J. Prog. Nucl. Magn. Res. Spect.* **1997**, *31*, 293−315.
(17) Kwim, W. p-Allyl systems in catalysis. In *Transition Metals in Homogeneous Catalysis*; Marcel Dekker Inc.: New York, 1971.
(18) Barkemeyer, J.; Haake, M.; Bargon, J. *J. Am. Chem. Soc.* **1995**, *117*, 2927−2928.
(19) *Annual Reports on NMR Spectroscopy*; Academic Press Inc.: San Diego, CA, 1993; Vol. *25*.
(20) Reineri, F.; Viale, A.; Giovenzana, G.; Santelia, D.; Dastrù, W.; Gobetto, R.; Aime, S. *J. Am. Chem. Soc.* **2008**, *130*, 15047−15053.
(21) (a) Johannesson, H.; Axelsson, O.; Karlsson, M. *C. R. Phys.* **2004**, *5*, 315−324. (b) Reineri, F.; Viale, A.; Dastrù, W.; Gobetto, R.; Aime, S. *Contrast Med. Mol. Imag.* **2010**, *6*, 77−84.
(22) Natterer, J.; Schedletzky, O.; Barkemeyer, J.; Bargon, J.; Glaser, S. J. *J. Magn. Reson.* **1998**, *133*, 92−97. Aime, S.; Gobetto, R.; Reineri, F.; Canet, D. *J. Chem. Phys.* **2003**, *119*, 8890−8896.
(23) Katz-Brull, R.; Degani, H. *Anticancer Res.* **1996**, *16*, 1375−1380.
(24) Cudalbu, C.; Comment, A.; Kurdzesau, F.; van Heeswijk, R. B.; Jannin, S.; Denisov, V.; Zirik, D.; Gruetter, R. *Phys. Chem. Chem. Phys.* **2010**, *15*, 5818−5823.